Zhong *et al. Insights into Imaging* (2023) 14:79
https://doi.org/10.1186/s13244-023-01426-5

Insights into Imaging
ESR EUROPEAN SOCIETY OF RADIOLOGY

ORIGINAL ARTICLE

Open Access

Robustness of radiomics features of virtual unenhanced and virtual monoenergetic images in dual-energy CT among different imaging platforms and potential role of CT number variability

Jingyu Zhong[1†], Zilai Pan[2†], Yong Chen[2], Lingyun Wang[2], Yihan Xia[2], Lan Wang[2], Jianying Li[3], Wei Lu[4], Xiaomeng Shi[5], Jianxing Feng[6], Fuhua Yan[2], Huan Zhang[2*] and Weiwu Yao[1*]

Abstract

Objectives To evaluate robustness of dual-energy CT (DECT) radiomics features of virtual unenhanced (VUE) image and virtual monoenergetic image (VMI) among different imaging platforms.

Methods A phantom with sixteen clinical-relevant densities was scanned on ten DECT platforms with comparable scan parameters. Ninety-four radiomic features were extracted via Pyradiomics from VUE images and VMIs at energy level of 70 keV (VMI_{70keV}). Test–retest repeatability was assessed by Bland–Altman analysis. Inter-platform reproducibility of VUE images and VMI_{70keV} was evaluated by coefficient of variation (CV) and quartile coefficient of dispersion (QCD) among platforms, and by intraclass correlation coefficient (ICC) and concordance correlation coefficient (CCC) between platform pairs. The correlation between variability of CT number radiomics reproducibility was estimated.

Results 92.02% and 92.87% of features were repeatable between scan–rescans for VUE images and VMI_{70keV}, respectively. Among platforms, 11.30% and 28.39% features of VUE images, and 15.16% and 28.99% features of VMI_{70keV} were with CV < 10% and QCD < 10%. The average percentages of radiomics features with ICC > 0.90 and CCC > 0.90 between platform pairs were 10.00% and 9.86% in VUE images and 11.23% and 11.23% in VMI_{70keV}. The CT number inter-platform reproducibility using CV and QCD showed negative correlations with percentage of the first-order radiomics features with CV < 10% and QCD < 10%, in both VUE images and VMI_{70keV} (r^2 0.3870–0.6178, all $p < 0.001$).

Conclusions The majority of DECT radiomics features were non-reproducible. The differences in CT number were considered as an indicator of inter-platform DECT radiomics variation.

Critical relevance statement: The majority of radiomics features extracted from the VUE images and the VMI70keV were non-reproducible among platforms, while synchronizing energy levels of VMI to reduce the CT number value variability may be a potential way to mitigate radiomics instability.

†Jingyu Zhong and Zilai Pan contributed equally to this work and share co-first authorship.

*Correspondence:
Huan Zhang
huanzhangy@163.com; zh10765@rjh.com.cn
Weiwu Yao
yaoweiwuhuan@163.com; yww4142@shtrhospital.com
Full list of author information is available at the end of the article

Key points

- The repeatability of DECT radiomics features was high between scan–rescans.
- The inter-reproducibility of radiomics features in VUE images and VMI_{70keV} was low.
- The differences in DECT techniques obviously altered the radiomics features.
- Synchronizing energy levels of VMI can potentially improve radiomics robustness.

Keywords Machine learning, Multidetector computed tomography, Reproducibility of results, Image enhancement, Image reconstruction

Graphical Abstract

Robustness of radiomics features of virtual unenhanced and virtual monoenergetic images in dual-energy CT among different imaging platforms and potential role of CT number variability

Insights into Imaging

EUROPEAN SOCIETY OF RADIOLOGY

- The repeatability of DECT radiomics features was high between scan-rescans.
- The inter-reproducibility of radiomics features in VUE images and VMI_{70keV} was low.
- The differences in DECT techniques obviously altered the radiomics features.
- Synchronizing energy levels of VMI can potentially improve radiomics robustness.

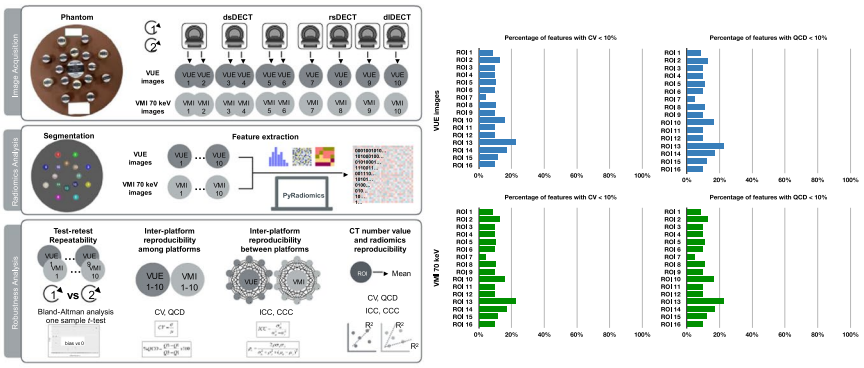

The majority of radiomics features extracted from the VUE images and the VMI_{70keV} were non-reproducible among platforms, while synchronizing energy levels of VMI to reduce the CT number value variability may be a potential way to mitigate radiomics instability.

Insights Imaging (2023) Zhong J, Pan Z, et al. DOI: 10.1186/s13244-023-01426-5

Introduction

Radiomics extracts minable data from medical images to answer diagnostic, prognostic, and predictive questions, with the aim to deliver precision medicine [1–5]. Although numerous studies have shown its potential for clinical decision-making, gap between promising the academic results and the clinical utilization still exists due to instability of radiomics features [6–9]. The robustness of radiomics features has been demonstrated to be sensitive and fragile to variations of data acquisition, image reconstruction, segmentation, image processing, and radiomics feature computation. The standardization of features is considered critical to overcome the difficulty in generalizability of radiomics [10], while it is still an open question which factors should be emphasized for improving radiomics robustness.

Dual-energy CT (DECT) is a tremendous innovation in CT technology that allows creation of numerous imaging datasets by enabling discrete acquisitions at more than one energy level [11, 12]. This technology has been coupled with radiomics and yielded as a superior imaging

biomarker with encouraging initial results in both oncological and non-oncological fields [13–17]. However, an important prerequisite for widespread application of radiomics on DECT data is a high degree of stability, calling for comprehensive investigation of which factors that influence on DECT radiomics robustness. Difference in single-energy CT (SECT) technique and diverse approaches of DECT acquisition result in CT number variation, and this variation is considered as an important underlying source of radiomics variation [18–21]. Meanwhile, the CT number values also diverge in virtual unenhanced (VUE) images and in virtual monoenergetic images (VMI) across DECT platforms [22, 23]. The energy level of VMI has impact on radiomics robustness [24, 25], and high repeatability of radiomics features could remain stable when the same equivalent energy level was used for VMI generation with different DECT approaches [26]. Accordingly, we hypothesized that the inter-platform variability of radiomic features due to differences in DECT data acquisition and reconstruction may be reduced by creating VMI at appropriate energy levels with comparable CT number values.

In this study, we therefore aimed to evaluate the inter-platform reproducibility of DECT radiomics features in the VUE images and the VMI at energy level of 70 keV (VMI_{70keV}) and explore whether variability of CT number value has correlation with the robustness of DECT radiomics features.

Materials and methods

Phantom

Figure 1 presents the workflow of this study. The institution's ethics approval was not required since this was a phantom study. A CT Dual-Energy Phantom Model (Gmamex, Gammex Inc.) was used. This phantom was composed of a 330-mm-in-diameter disk of water-equivalent material and sixteen 28-mm-in-diameter holes for holding interchangeable inserts of various clinical-relevant densities. We selected five iodine inserts with concentrations from 2.0 to 15.0 mg/mL, and eleven rods with densities of 0.44–1.69 g/cm^3, mimicking wide range of CT number values of human tissues. The inserts were placed to minimize beam-hardening artifacts and kept unchanged across all scans.

Image acquisition and reconstruction

The phantom was scanned on ten DECT imaging platforms using seven DECT-capable scanners with comparable acquisition and reconstruction parameters (Table 1). Three types of DECT scanners were employed in our study, namely dual-source DECT (dsDECT), rapid kV-switching DECT (rsDECT), and dual-layer detector DECT (dlDECT), to generate images that were comparable to conventional SECT 120-kVp images. Three dsDECT scanners were used, each with two different tube voltage combinations for data acquisition, to provide six DECT imaging platforms. Three rsDECT scanners were used to provide three DECT imaging platforms. One dlDECT scanner at tube voltage of 120 kVp was used to provide the tenth DECT imaging platform. The scan field of view (500×500 mm), reconstruction matrix (512×512), and slice thickness (5 mm) remained the same for all acquisitions to keep voxel size unchanged. The volume CT dose index, strength of iteration reconstruction algorithm, and reconstruction kernel were chosen to present the typical abdomen-pelvic examinations at our institution. Each scan was repeated several minutes apart with repositioning, to allow test–retest repeatability analysis.

Two kinds of images were generated on each DECT imaging platform for radiomic robustness assessment, namely the VUE image and the VMI_{70keV}. The VUE images were selected to show the impact of differences in material decomposition techniques between platforms. The VUE images were created using proprietary DECT software tools per vendor-specific material decomposition techniques: Advantage Workstation version 4.7 (GE Healthcare), Syngo.via version VB10 (Siemens Healthineer), and IntelliSpace Portal Workstation version 10 (Philips Healthcare), respectively. The VMI_{70keV} were generated as a gray-scaled, contrast-enhanced benchmark reconstruction relying on comparable linear energy blending approaches on each platform [27–29].

Segmentation and feature extraction

We applied an open-source ITK-SNAP software version 3.6.0 (http://www.itksnap.org/pmwiki/pmwiki.php) for segmentation, following a rigid registration to minimize variations [30]. Sixteen circular regions-of-interest (ROIs) of 26 pixels (25 mm) in diameter were placed at the center of each insert to present the clinical-relevant densities. To present the true difference among platforms, we did not employ any image preprocessing steps. Python version 3.7.6 (https://www.python.org) with Image Biomarker Standardization Initiative (IBSI)-compliant Pyradiomics package version 3.0 (https://pyradiomics.readthedocs.io/en/latest/) was used to extract the radiomics features from the original images [31]. Since the ROIs were fixed, we excluded the 26 shape-based features. Consequently, 94 radiomics features were extracted from each ROI, namely 19 order features and 75 texture features. The detailed radiomics analysis methods are presented in Additional file 1: Note S1.

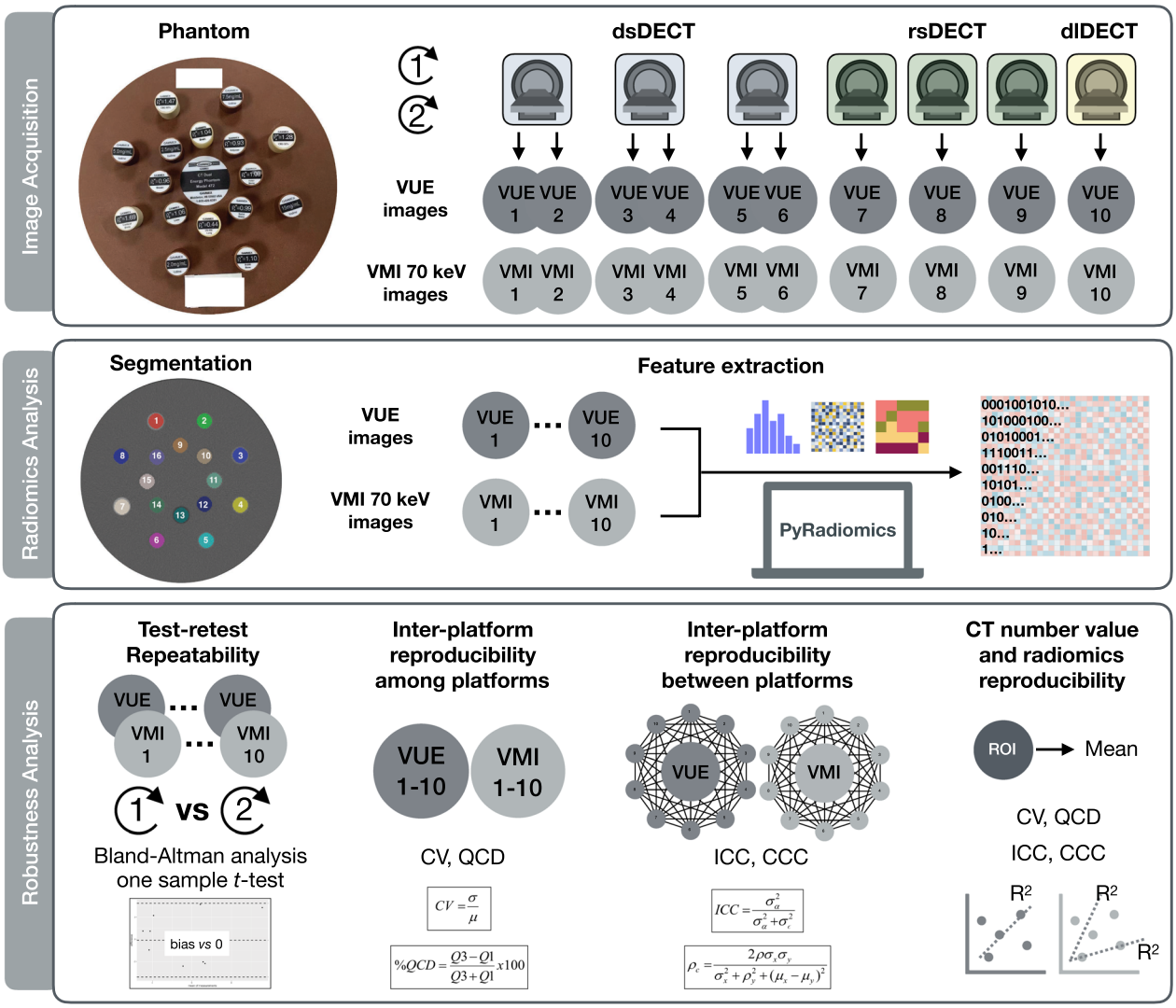

Fig. 1 Study workflow. This study was composed of three steps, namely image acquisition, radiomics analysis and robustness analysis. A standardized phantom was scanned on ten platforms on seven DECT-capable scanners of three types with the same voxel and typical abdomen-pelvic examination parameters. Corresponding VUE images and VMI_{70keV} were generated. Pyradiomics was employed to extract 19 first-order and 75 texture radiomics features from ROIs segmented with a rigid registration. The test–retest repeatability was evaluated by Bland–Altman analysis for repeated scans, and the hypothesis that the obtained biases of the radiomics feature values between the scan and rescan was equal to zero was tested by one-sample *t* test. The inter-platform reproducibility among VUE images, and that among VMI_{70keV} images, were assessed by CV and QCD. Inter-platform reproducibility between two particular platform pairs were estimated by ICC and CCC to characterize inter-platform difference across DECT platforms. Since there were ten platforms, forty-five comparisons were performed within the VUE images and within the VMI_{70keV}, respectively. CT number and their inter-platform reproducibility were calculated. The correlation between CT number variability of and percentage of robust radiomics features was investigated. dsDECT = dual-source dual-energy CT, rsDECT = rapid kV-switching dual-energy CT, dlDECT = dual-layer dual-energy CT

Radiomics robustness analysis

To present the radiomics robustness, the test–retest repeatability and the inter-platform reproducibility were estimated [32]. The test–retest repeatability was assessed using images from repeating scans by Bland–Altman analysis [33]. The percentage of repeatable features was calculated, with a cutoff value of 90% of 16 ROIs [18], indicating the portion of feature scan–rescan measurements that did not exceed the 95% limits of agreement. To test the hypothesis that the obtained biases of the radiomics feature values between the scan and rescan was equal to zero, a one-sample *t* test was performed.

Table 1 Dual-energy CT acquisition and reconstruction parameters

No. of platform	Vendor	Scanner	Type	Tube Voltage (kVp)	Milliamperage (mA or mAs)	Rotation Time (sec)	Volume CT dose index (mGy)	Iteration Method	Reconstruction kernel
1	SIEMENS	SOMATOM Drive	dsDECT	80/140	580/224	0.5	20.00	ADMIRE 2	Q40f
2	SIEMENS	SOMATOM Drive	dsDECT	100/140	279/216	0.5	20.04	ADMIRE 2	Q40f
3	SIEMENS	SOMATOM Definition Flash	dsDECT	80/140	531/205	1.0	20.01	SAFIRE 2	Q40s
4	SIEMENS	SOMATOM Definition Flash	dsDECT	100/140	258/199	1.0	19.96	SAFIRE 2	Q40s
5	SIEMENS	SOMATOM Force	dsDECT	70/150	848/212	0.5	20.00	ADMIRE 2	Qr40
6	SIEMENS	SOMATOM Force	dsDECT	100/150	294/147	0.5	20.02	ADMIRE 2	Qr40
7	GE	Discovery CT750 HD	rsDECT	80/140	640*	0.6	21.84	ASiR-V 40%	Standard
8	GE	Revolution Apex	rsDECT	80/140	370*	1.0	19.75	ASiR-V 40%	Standard
9	GE	Revolution CT	rsDECT	80/140	275*	0.8	20.00	ASiR-V 40%	Standard
10	PHILIPS	IQon spectral CT	dlDECT	120	221	0.75	20.00	iDOSE 3	Standard (B)

* represents mA not mAs for GE medical systems. *dsDECT* dual-source dual-energy CT, *rsDECT* rapid kV-switching dual-energy CT, *dlDECT* dual-layer dual-energy CT

The inter-platform reproducibility among the VUE images from ten platforms, and that among the VMI_{70keV} from ten platforms were evaluated, by the coefficient of variation (CV) [34] and the quartile coefficient of dispersion (QCD) [35], respectively, with a cutoff of 10% [30]. To further characterize inter-platform difference across DECT platforms, the inter-platform reproducibility between each platform within the VUE images and within the VMI_{70keV} was estimated to present consistency of two particular platforms, using the intraclass correlation coefficient (ICC) of single rater, absolute agreement, two-way random effects model [36] and the concordance correlation coefficient (CCC) [37, 38], with a cutoff of 0.90 [39, 40]. Since there were ten platforms, forty-five pairs of platforms within the VUE images and within the VMI_{70keV} were compared, respectively, which resulted in ninety comparisons in total. Additional attention was paid to the reproducibility of fourteen individual radiomics features that are important as biomarkers in clinical studies and have been reported to be robust [41–43]. The CT number values and their inter-platform reproducibility were calculated.

Statistical analysis

The statistical analysis was performed with R language version 4.1.3 (https://www.r-project.org/) within RStudio software version 1.4.1106 (https://www.rstudio.com/). The continuous variables were presented as average ± standard deviation (SD). Proportions of robust features were indicated as percentages. The correlation between inter-platform CT number reproducibility and percentage of radiomics features that met the criteria of reproducibility was quantitatively estimated by Spearman correlation analysis due to the nonnormal distribution of the data. A two-sided p value < 0.05 was considered as statistically significant. The detailed statistical analysis methods are presented in Additional file 1: Note S2.

Results

Test–retest repeatability analysis of radiomics features

The average percentages ± SD of repeatable radiomics features were 92.02 ± 7.43% and 92.87 ± 4.71% for the VUE images and the VMI_{70keV}, respectively, when the cutoff value was 90% of 16 ROIs (Additional file 1: Table S1 and Fig. S1). The biases of the radiomics feature values between the scan and rescan were not significantly different from zero (all $p > 0.05$).

Inter-platform radiomics reproducibility among all platforms within the VUE images and within the VMI_{70keV}

The average percentages ± SD of inter-platform reproducible radiomics features were 11.30 ± 4.15% and 28.39 ± 7.19% among all platforms within the VUE images, and 15.16 ± 3.99% and 28.99 ± 13.36% among all platforms within the VMI_{70keV}, respectively, when

Table 2 Inter-platform reproducibility of radiomics among all platforms within the VUE images and within the VMI_{70keV}

Feature class	CV < 10%		CV mean		QCD < 10%		QCD mean	
	VUE (%)	VMI_{70keV} (%)	VUE	VMI_{70keV}	VUE (%)	VMI_{70keV} (%)	VUE	VMI_{70keV}
First order (19 features)	8.88	26.64	0.5007	0.7358	44.74	50.99	0.4037	0.2484
Texture (75 features)	19.83	20.58	0.4232	0.4042	41.25	38.67	0.2791	0.2625
GLCM (24 features)	16.93	16.15	0.5460	0.4878	30.21	28.91	0.4073	0.3402
GLDM (14 features)	20.54	20.54	0.3081	0.3151	30.36	29.46	0.1839	0.1923
GLRLM (16 features)	7.03	7.03	0.3716	0.3602	25.39	21.48	0.2156	0.2244
GLSZM (16 features)	5.47	8.20	0.3975	0.3966	14.84	15.23	0.2482	0.2558
NGTDM (5 features)	0.00	0.00	0.4024	0.4176	5.00	12.50	0.2328	0.2299
Overall (94 features)	11.30	15.16	0.4388	0.4712	28.39	28.99	0.3043	0.2597

Percentage indicates the percentage of features met the cutoffs for robustness measures (CV < 10% and QCD < 10%). *GLCM* Gray-level co-occurrence matrix, *GLDM* Gray-level dependence matrix, *GLRLM* Gray-level run-length matrix, *GLSZM* Gray-level size zone matrix, *NGTDM* Neighborhood gray-tone difference matrix

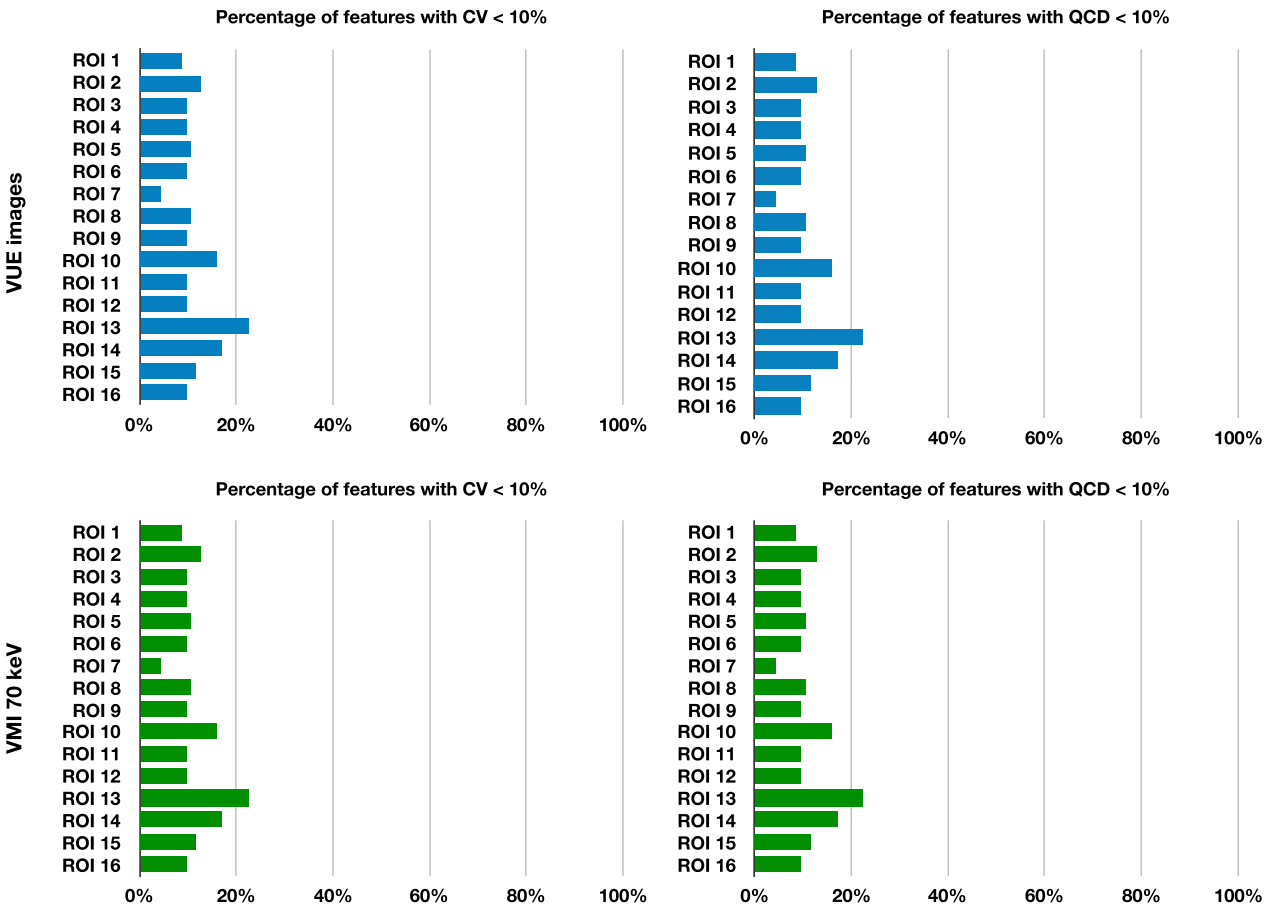

Fig. 2 Inter-platform reproducibility of radiomics among all platforms within the VUE images and within the VMI_{70keV}. Upper left and right graphs showed percentages of radiomic features that were deemed as inter-platform reproducible among platforms within the VUE images per CV < 10% and QCD < 10%, respectively, according to ROIs. Lower left and right graphs showed percentages of radiomic features that were deemed as inter-platform reproducible among platforms within the VMI_{70keV} per CV < 10% and QCD < 10%, respectively, according to 16 ROIs

the criteria were CV < 10% and QCD < 10% (Table 2 and Fig. 2). The percentages of radiomics features that met the reproducible criteria ranged from 4.26 to 22.34% for CV < 10% and from 17.02 to 38.30% for QCD < 10% in VUE images, and varied from 9.57 to 20.21% for CV < 10% and from 19.15 to 38.30% for QCD < 10%

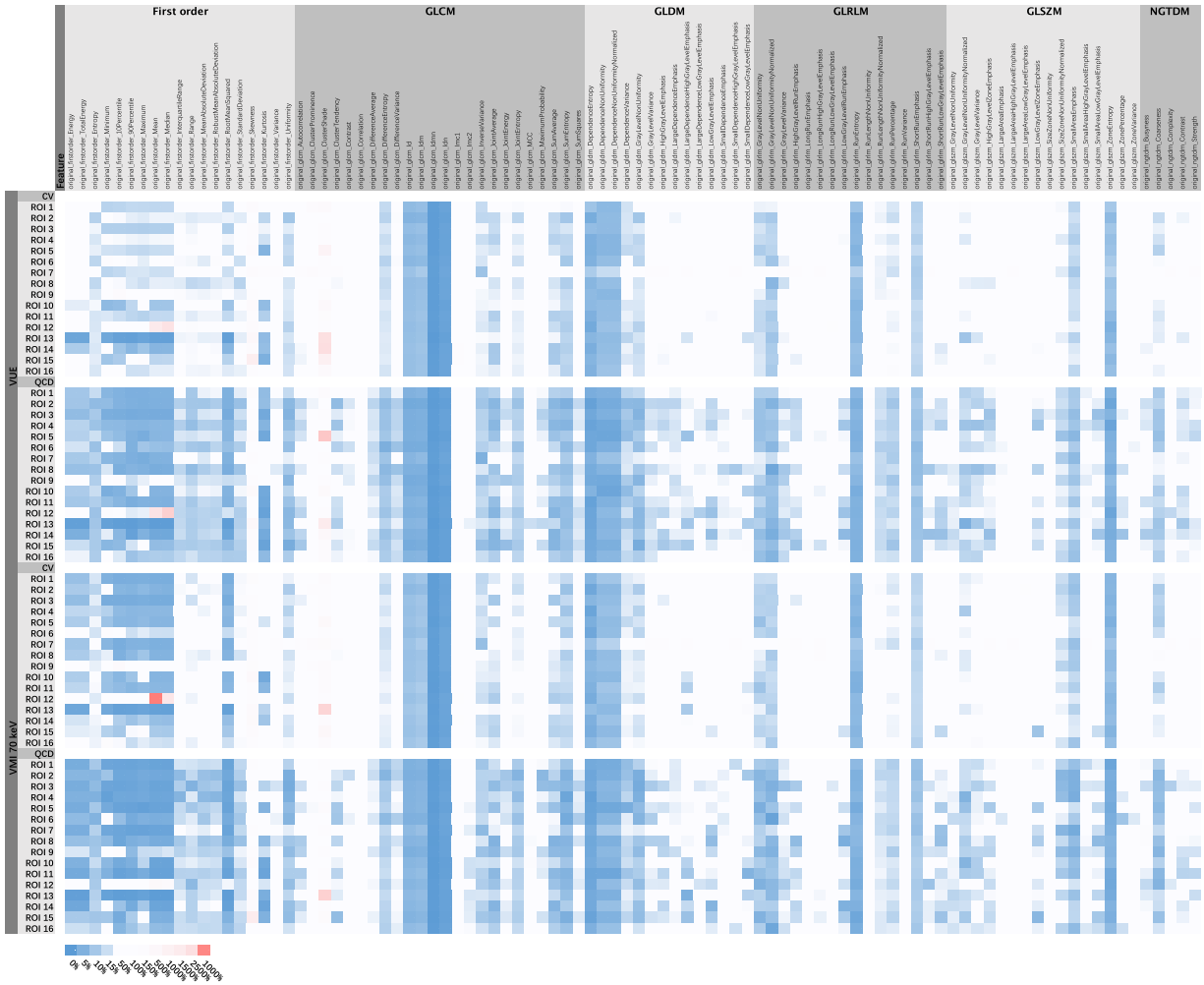

Fig. 3 Heatmap of Inter-platform reproducibility of radiomics among all platforms within the VUE images and within the VMI_{70keV}. Percentages indicated CV values and QCD values. GLCM = gray-level co-occurrence matrix, GLDM = gray-level dependence matrix, GLRLM = gray-level run-length matrix, GLSZM = gray-level size zone matrix, NGTDM = neighborhood gray-tone difference matrix

Table 3 Inter-platform reproducibility of radiomics between each platform within the VUE images and within the VMI_{70keV}

Feature class	ICC > 0.90		ICC mean		CCC > 0.90		CCC mean	
	VUE (%)	VMI_{70keV} (%)	VUE	VMI_{70keV}	VUE (%)	VMI_{70keV} (%)	VUE	VMI_{70keV}
First order (19 features)	45.03	49.36	0.6654	0.6811	44.68	49.36	0.6584	0.6749
Texture (75 features)	1.13	1.57	0.2324	0.2782	1.04	1.57	0.2247	0.2695
GLCM (24 features)	1.39	2.96	0.2871	0.3146	1.39	2.96	0.2782	0.3050
GLDM (14 features)	1.27	0.95	0.2093	0.2724	1.11	0.95	0.2028	0.2645
GLRLM (16 features)	0.97	0.97	0.2083	0.2644	0.69	0.97	0.2009	0.2560
GLSZM (16 features)	0.69	0.97	0.1963	0.2455	0.69	0.97	0.1895	0.2377
NGTDM (5 features)	1.33	0.44	0.2262	0.2681	1.33	0.44	0.2181	0.2588
Overall (94 features)	10.00	11.23	0.3199	0.3596	9.86	11.23	0.3124	0.3515

Percentage indicates the percentage of features met the cutoffs for robustness measures (ICC > 0.90 and CCC > 0.90). *GLCM* Gray-level co-occurrence matrix, *GLDM* Gray-level dependence matrix, *GLRLM* Gray-level run-length matrix, *GLSZM* Gray-level size zone matrix, *NGTDM* Neighborhood gray-tone difference matrix

in VMI_{70keV}, according to ROIs (Additional file 1: Table S2). The individual radiomics features showed variable reproducibility (Fig. 3), and the top ten most inter-platform reproducible features among the VUE images and the VMI_{70keV} were mainly the texture features (36 out of 40; Additional file 1: Table S3). The reproducibility of fourteen important radiomics features did not show high reproducibility neither in VUE images (CV values 16.64–579.47%, QCD values 9.11–519.92%) nor in VMI_{70keV} images (CV values 17.61–426.45%, QCD values 9.28–352.37%) (Additional file 1: Table S4).

Inter-platform radiomics reproducibility between platform pairs within the VUE images and within the VMI_{70keV}

The average percentages ± SD of inter-platform reproducible radiomics features were 10.01 ± 3.79% and 9.86 ± 3.67% between each platform within the VUE images, and 11.23 ± 5.78% and 11.23 ± 5.78% within the VMI_{70keV}, respectively, when the criteria were ICC > 0.90 and CCC > 0.90 (Table 3 and Fig. 4). The percentages of radiomics features that met the reproducible criteria ranged from 1.06 to 26.60% for ICC > 0.90 and from 1.06 to 24.47% for CCC > 0.90 in VUE images and varied from 9.57 to 40.43%% for ICC > 0.90 and from 9.57 to 41.49% for CCC > 0.90 in VMI_{70keV}, according to comparisons (Additional file 1: Table S5 and Fig. S2). The individual radiomics features showed variable reproducibility (Additional file 1: Fig. S3), the top ten most inter-platform reproducible features between each platform within the VUE images and the VMI_{70keV} were mainly the first-order features (36 out of 40; Additional file 1: Table S6). The reproducibility of fourteen important radiomics features did not show high reproducibility neither in VUE images (ICC values, 0.0918–0.4368, CCC values 0.0948–0.4235) nor in VMI_{70keV} images (ICC values 0.0948–0.4469, CCC values 0.0938–0.4345) (Additional file 1: Table S7).

Table 4 Inter-reproducibility of CT number values

Images	Criteria			
Inter-platform reproducibility among all platforms within the VUE images and within the VMI_{70keV}				
16 ROIs	CV < 10%	CV mean	QCD < 10%	QCD mean
VUE	18.75%	1.1389	81.25%	1.4144
VMI_{70keV}	68.75%	6.8006	87.50%	0.3055
Inter-platform reproducibility between particular platforms within the VUE images and within the VMI_{70keV}				
45 Comparisons	ICC > 0.90	ICC mean	CCC > 0.90	CCC mean
VUE	95.56%	0.9803	95.56%	0.9803
VMI_{70keV}	100.00%	0.9974	100.00%	0.9972

Percentage indicates the percentage of features met the cutoffs for robustness measures (CV < 10% and QCD < 10%, ICC > 0.90 and CCC > 0.90)

CT number values and radiomics reproducibility

The CT number values varied among platforms within the VUE images and the VMI_{70keV} (Table 4 and Additional file 1: Table S8). The reproducibility of CT number values and percentage of first-order radiomics features that met the criteria of reproducibility showed correlations (Additional file 1: Fig. S4). The negative correlations were found using CV and QCD in both VUE images

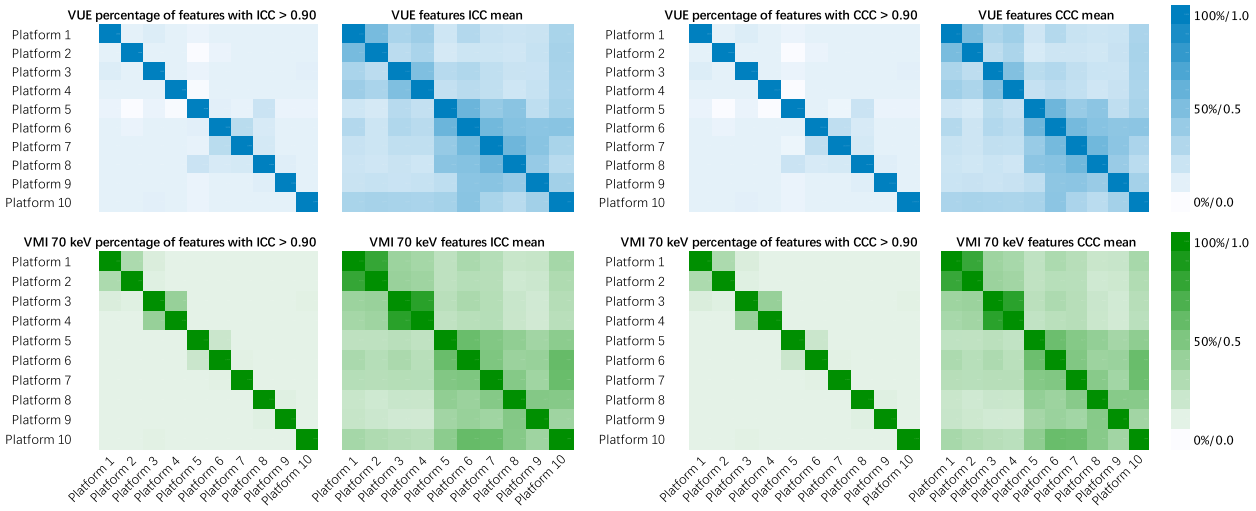

Fig. 4 Inter-platform reproducibility of radiomics between platform pairs within the VUE images and within the VMI_{70keV}. Upper graphs showed percentages of radiomic features that were deemed as inter-platform reproducible between each platform per ICC > 0.90 and CCC > 0.90, and the mean of ICC and CCC between each platform within the VUE images, respectively, according to 45 comparisons. Lower graphs showed percentages of radiomic features that were deemed as inter-platform reproducible between each platform per ICC > 0.90 and CCC > 0.90, and the mean of ICC and CCC between each platform within the VMI_{70keV}, respectively, according to 45 comparisons

and VMI_{70keV} (r^2 0.3870–0.6178, all $p < 0.001$), and positive correlations were estimated using ICC ($r^2 = 0.7378$, $p < 0.001$) and CCC ($r^2 = 0.7717$, $p < 0.001$) in the VUE images (Additional file 1: Fig. S4).

Discussion

Our study investigated the test–retest repeatability and the inter-platform reproducibility of the VUE images and the VMI_{70keV} in DECT among different platforms, using data from a phantom with inserts of clinical-relevant multiple densities. Our finding demonstrated that the test–retest repeatability of radiomics features derived from different DECT platforms was high, but the inter-platform reproducibility was relatively low, indicating the potential influence of various DECT acquisition and reconstruction techniques. We further characterized the inter-platform difference across DECT platforms by comparing different platform pairs and found that their reproducibility varied according to platforms. The differences in CT number values were deemed to have relation with the inter-platform reproducibility of DECT radiomics features, indicating the potential role of CT number values as an indicator in synchronizing the energy level of VMI of different DECT platforms to improve DECT radiomics robustness.

Our study showed that 11.30% and 28.39% and 15.16% and 28.99% of features were with CV < 10% and QCD < 10%, among the VUE images and the VMI_{70keV} of different DECT platforms, respectively, suggesting the difference in DECT acquisition and reconstruction techniques could be a source of instability. A previous study presented that 17.09% and 27.73% of radiomics features were considered to be reproducible among SECT platforms [18]. This did not support the hypothesis that the differences in DECT data acquisition and reconstruction between platforms may introduce greater variability of radiomic features compared to SECT with a more similar technical set-up [19]. However, in terms of reproducibility, the images acquired via different SECT and DECT platforms, as well as the VUE images and the VMI generated from different DECT platforms, should not be used interchangeably in radiomic studies, even if they were scanned with comparable parameters.

The inter-platform reproducibility between each platform within the VUE images and within the VMI_{70keV} presented varying percentage of radiomics features that met the reproducible criteria. A previous study showed 0.00% and 0.00% of phantom-derived features with CCC > 0.90 in the VUE images and the VMI_{65keV}, respectively, between different DECT scanner types, while 2.45–16.15% and 2.71–11.11% of patient-derived features were estimated with CCC > 0.90 in the VUE images and the VMI_{65keV}, respectively [19]. The highest percentage of reproducible features were achieved between a third-generation dsDECT scanner and a rsDECT scanner [19]. Another phantom study showed that 66.6–83.5% of radiomics features were with CCC > 0.90 between a third-generation dsDECT scanner and a split-filter DECT scanner within the VMI of the same energy level from 40 to 190 keV [26]. Our study supported that a third-generation dsDECT scanner shared more in common with rsDECT scanners, but did not find similarity between second-generation dsDECT scanners and rsDECT scanners. Indeed, two second-generation dsDECT scanners with two combinations of tube voltages showed high reproducibility. Although the variability among DECT scanners was not greater than that among SECT scanners, the differences in DECT data acquisition and reconstruction between platforms did introduce variability among DECT imaging platforms.

In addition to the overall reproducibility evaluations of radiomics features, we also investigated fourteen individual radiomics features that are currently of interest in clinical research and have been reported to be robust to quantum noise, segmentation variability, and image acquisition [41–43]. However, these radiomics features did not show high reproducibility among DECT platforms, indicating that mitigation of DECT-specific radiomics variability was of importance for generalizability of radiomics models derived from one DECT platform to the other.

The texture features occupied the majority of the top ten most inter-platform reproducible features among the VUE images and among the VMI_{70keV} using CV or QCD as metrics, while the reproducible features between each platform using ICC or CCC were mainly the first-order features. One of the important sources of the inter-platform variability of radiomics is CT number values [18]. The metrics of CV and QCD is considered to present the overall difference among platforms. The outliers of CT number values may have greater impact on the first-order features. Our study found that most of the texture features that survived CV and QCD analysis were related to the homogeneity of the ROI. They were more sensitive to the small noise within ROI than the variations of CT number values. Therefore, the influence of the unstable CT number values on the texture features was less than that on the first-order features. On the other hand, the metrics of ICC and CCC allow evaluation between two specific platforms. The platform five, with obvious differences in CT number values, showed lower reproducibility of the first-order features comparing to other DECT platforms, indicating that the key for improving

the reproducibility of first-order features was to keep CT number values stable. In other words, it is possible to improve radiomics reproducibility between DECT platforms by minimizing variability of CT number values, especially the first-order features.

To the best of our knowledge, our study is the first to show the correlation between variability of CT number value and reproducibility of the first-order features derived from DECT data. It is not strange that the first-order features, but not the texture features, were strongly platform-dependent, since the first-order features were more sensitive to difference of CT number values among platforms. It has been considered as a source of difference of radiomics features in SECT that the variability of CT number values across scanners due to the different X-ray spectra of different scanners [20], as well as additional slight differences of the images caused by different calibrations method [30]. CT number values are simple representations of the different imaging appearances, texture features, and quantitative capabilities of DECT images with different technical approaches [11, 12, 22, 23] and may lead to variations among DECT platforms.

CT number values potentially serve as an indicator for improvement for reproducibility among DECT platforms. The lower the variability of CT number values among platforms achieved, the higher the inter-platform reproducibility of the first-order features became. Unlike the VUE images, the VMI could provide an increasing trend of CT number values with decreasing energy level [24]. Meanwhile, the VMI showed lower variability in CT number values than VUE images, when comparable acquisition and reconstruction settings were used [22, 23]. This result might provide insights for reducing the inter-platform difference in DECT radiomic features by better synchronizing energy levels of VMI according to CT number values. It would be more practicable for clinical practice to compare the CT number values, because it is time-consuming to calculate reproducibility of high-dimensional radiomics data extracted from all available energy level of VMIs from different DECT platforms. Future studies should explore the utility of CT number values as an indicator for synchronizing energy level of VMI to improve DECT radiomics robustness.

Additionally, the use of VMI could potentially open more possibilities for radiomics modeling with its flexibility to calculate at low energy level to increase contrast and iodine attenuation or to compute at high energy level to reduce beam-hardening artefacts [44, 45]. The energy level of 70 keV was chosen because this was used as a clinical standard of reference at our institution [18, 46] and has been suggested to be comparable to conventional images [27–29]. However, concerns remained on the potential impact of non-matching energy levels of VMI on radiomics features [24]. Although the choice of synchronized energy level of VMI improved reproducibility between platforms [26], it is still unknown whether the energy level of VMI could alter the underlying minable information. Initial study suggested that VMI at different energy levels could provide varying performance of radiomics models for different clinical tasks [26]. We believe that the choice of energy level of VMI should hence be made to balance radiomics robustness and the specific clinical task.

The implementation of a preprocessing step may be necessary to harmonize data from different platforms using varying DECT techniques. Recently, many preprocessing methods have been introduced into radiomics studies for improving reproducibility of radiomic features, including min–max normalization, z-score normalization, mean normalization, batch effect correction, pixel resampling, Butterworth filtering, ComBat harmonization, radiomics data harmonization models specific to different clinical tasks, etc. [47–54]. As shown in our study, without the preprocessing step, the DECT images are not comparable between platforms in terms of radiomic features. These preprocessing methods have potential to improve the reproducibility of radiomic features among DECT platforms, while their influence on the CT values remains unknown. We believe future studies should test these preprocessing methods to find out which can harmonize data from different platforms using different dual-energy techniques while maintaining CT values.

Our study has limitations that need to be acknowledged. First, we did not investigate the robustness of radiomic features extracted from tumors, but rather from phantom of homogeneous clinical-relevant densities. Our results may not be directly translated to clinical practice, partly due to lacking of texture [18, 46]. However, the phantom allows more specific results in humans benefiting by its similarity to human density [55]. Second, we did not identify at which energy levels of VMIs to accomplish the highest inter-platform reproducibility. Nevertheless, our findings showed the possibility of harmonizing inter-platform radiomics features by synchronizing energy levels of VMIs and showed the potential role of CT number values in guiding selection of energy levels for this purpose. With multiple phantom scans on different platforms, one may be able to adjust energy levels of different imaging platforms to obtain similar CT number values for the same object. Therefore, a pre-calibrated lookup table may be possible to account for the differences of data acquisition and image reconstruction from different DECT platforms to

improve DECT-derived radiomics robustness. Third, we only investigated fourteen individual radiomics features in detail. These radiomics features were considered to be clinically important, but the ability of radiomics features for clinical interpretation or classification varied according to specific tasks. Therefore, further studies with patient images on specific clinical applications are warranted. Last, the results of our study should be carefully interpreted as hypothesis generating. We neither perform experiments to test the feasibility of CT numbers as a correction factor for reducing inter-platform variability nor conduct experiments to investigate the potential impact of a preprocessing step on the reproducibility of radiomics features. Our findings may provide insights on improvement of the inter-platform reproducibility, and our ongoing work is verifying the hypothesis.

To conclude, we have demonstrated that the radiomics features extracted from the VUE images and the VMI_{70keV} are not highly reproducible across different DECT platforms, despite using comparable acquisition and reconstruction parameters. DECT-derived radiomic models must be interpreted with caution due to the doubtful generalizability. The variability of CT number values is correlated with the reproducibility of the first-order features in radiomics, implying a potential way to mitigate radiomics instability among DECT platforms. Future studies should investigate the possibility of synchronizing energy levels of VMI among different DECT platforms with an appropriate preprocessing step to improve the robustness of DECT-derived radiomics.

Abbreviations

CCC	Concordance correlation coefficient
CV	Coefficient of variation
DECT	Dual-energy computed tomography
dlDECT	Dual-layer detector dual-energy computed tomography
dsDECT	Dual-source dual-energy computed tomography
ICC	Intraclass correlation coefficient
QCD	Quartile coefficient of dispersion
ROI	Region of interest
rsDECT	Rapid kV-switching dual-energy computed tomography
SD	Standard deviation
SECT	Single-energy computed tomography
VMI	Virtual monoenergetic images
VUE	Virtual unenhanced images

Supplementary Information

The online version contains supplementary material available at https://doi.org/10.1186/s13244-023-01426-5.

Additional file 1. Supplementay Materials.

Acknowledgements
The authors would like to express their gratitude to Dr. Guangyao Wu for his suggestions on data interpretation, Prof. Baisong Wang for his suggestions on statistical analysis, and Dr. Shiqi Mao for his comments on data visualization.

Author contributions
All the authors contributed to the study concepts and design. JYZ and ZLP contributed to the literature research. JYZ, ZLP, YC, LYW, YHX, LW, and JXF contributed to the experimental studies and data analysis. JYZ, ZLP, and YC contributed to the statistical analysis. JYZ prepared the original version of manuscript preparation. All authors read and approved the final version of the manuscript. HZ and WWY supervised the whole study. WWY is the guarantor of the integrity of the entire study.

Funding
This study has received funding by National Natural Science Foundation of China (82271934), Shanghai Science and Technology Commission Science and Technology Innovation Action Clinical Innovation Field (18411953000), Yangfan Project of Science and Technology Commission of Shanghai Municipality (22YF1442400), Medicine and Engineering Combination Project of Shanghai Jiao Tong University (YG2019ZDB09, YG2021QN08), and Research Fund of Tongren Hospital, Shanghai Jiao Tong University School of Medicine (TRKYRC-XX202204), Guangci Innovative Technology Launch Plan of Ruijin Hospital, Shanghai Jiao Tong University School of Medicine (2022-13). The funders played no role in the study design, data collection or analysis, decision to publish, or manuscript preparation.

Availability of data and materials
All data generated or analyzed during this study are included in this published article and its supplementary information files.

Declarations

Ethics approval and consent to participate
Not applicable.

Consent for publication
Not applicable.

Competing interests
JYL and WL are employees of GE Healthcare (China). However, they neither had access nor control over the phantom data acquisition and analysis. JXF is employee of Haohua Technology Co., Ltd. (Shanghai, China). All other authors of this manuscript declare no relationships with any companies whose products or services may be related to the subject matter of the article.

Author details
[1]Department of Imaging, Tongren Hospital, Shanghai Jiao Tong University School of Medicine, Shanghai 200336, China. [2]Department of Radiology, Ruijin Hospital, Shanghai Jiao Tong University School of Medicine, Shanghai 200025, China. [3]Computed Tomography Research Center, GE Healthcare, Beijing 100176, China. [4]Computed Tomography Research Center, GE Healthcare, Shanghai 201203, China. [5]Department of Materials, Imperial College London, London SW7 2AZ, UK. [6]Haohua Technology Co., Ltd., Shanghai 201100, China.

Received: 18 February 2023 Accepted: 5 April 2023
Published online: 11 May 2023

References

1. Lambin P, Rios-Velazquez E, Leijenaar R et al (2012) Radiomics: extracting more information from medical images using advanced feature analysis. Eur J Cancer 48(4):441–446
2. Gillies RJ, Kinahan PE, Hricak H (2016) Radiomics: images are more than pictures, they are data. Radiology 278(2):563–577
3. O'Connor JP, Aboagye EO, Adams JE et al (2017) Imaging biomarker roadmap for cancer studies. Nat Rev Clin Oncol 14:169–186
4. Lambin P, Leijenaar RTH, Deist TM et al (2017) Radiomics: the bridge between medical imaging and personalized medicine. Nat Rev Clin Oncol 14(12):749–762
5. van Timmeren JE, Cester D, Tanadini-Lang S, Alkadhi H, Baessler B (2020) Radiomics in medical imaging-"how-to" guide and critical reflection. Insights Imaging 11(1):91

6. Park JE, Park SY, Kim HJ, Kim HS (2019) Reproducibility and generalizability in radiomics modeling: possible strategies in radiologic and statistical perspectives. Korean J Radiol 20(7):1124–1137
7. Zwanenburg A (2019) Radiomics in nuclear medicine: robustness, reproducibility, standardization, and how to avoid data analysis traps and replication crisis. Eur J Nucl Med Mol Imaging 46(13):2638–2655
8. Cattell R, Chen S, Huang C (2019) Robustness of radiomic features in magnetic resonance imaging: review and a phantom study. Vis Comput Ind Biomed Art 2(1):19
9. Pfaehler E, Zhovannik I, Wei L et al (2021) A systematic review and quality of reporting checklist for repeatability and reproducibility of radiomic features. Phys Imaging Radiat Oncol 20:69–75
10. Zwanenburg A, Vallières M, Abdalah MA et al (2020) The image biomarker standardization initiative: standardized quantitative radiomics for high-throughput image-based phenotyping. Radiology 295(2):328–338
11. McCollough CH, Leng S, Yu L, Fletcher JG (2015) Dual- and multi-energy CT: principles, technical approaches, and clinical applications. Radiology 276(3):637–653
12. Parakh A, Lennartz S, An C et al (2021) Dual-energy CT images: pearls and pitfalls. Radiographics 41(1):98–119
13. Homayounieh F, Singh R, Nitiwarangkul C et al (2020) Semiautomatic segmentation and radiomics for dual-energy CT: a pilot study to differentiate benign and malignant hepatic lesions. AJR Am J Roentgenol 215(2):398–405
14. DodaKhera R, Homayounieh F, Lades F et al (2020) Can dual-energy computed tomography quantitative analysis and radiomics differentiate normal liver from hepatic steatosis and cirrhosis? J Comput Assist Tomogr 44(2):223–229
15. Wang L, Zhang Y, Chen Y et al (2021) The performance of a dual-energy CT derived radiomics model in differentiating serosal invasion for advanced gastric cancer patients after neoadjuvant chemotherapy: iodine map combined with 120-kV equivalent mixed images. Front Oncol 10:562945
16. Chen Y, Yuan F, Wang L et al (2022) Evaluation of dual-energy CT derived radiomics signatures in predicting outcomes in patients with advanced gastric cancer after neoadjuvant chemotherapy. Eur J Surg Oncol 48(2):339–347
17. An C, Li D, Li S et al (2022) Deep learning radiomics of dual-energy computed tomography for predicting lymph node metastases of pancreatic ductal adenocarcinoma. Eur J Nucl Med Mol Imaging 49(4):1187–1199
18. Chen Y, Zhong J, Wang L et al (2022) Robustness of CT radiomics features: consistency within and between single-energy CT and dual-energy CT. Eur Radiol 32(8):5480–5490
19. Lennartz S, O'Shea A, Parakh A, Persigehl T, Baessler B, Kambadakone A (2022) Robustness of dual-energy CT-derived radiomic features across three different scanner types. Eur Radiol 32(3):1959–1970
20. Chen-Mayer HH, Fuld MK, Hoppel B et al (2017) Standardizing CT lung density measure across scanner manufacturers. Med Phys 44(3):974–985
21. Mackin D, Fave X, Zhang L et al (2015) Measuring computed tomography scanner variability of radiomics features. Invest Radiol 50(11):757–765
22. Lennartz S, Parakh A, Cao J, Zopfs D, GroßeHokamp N, Kambadakone A (2021) Inter-scan and inter-scanner variation of quantitative dual-energy CT: evaluation with three different scanner types. Eur Radiol 31(7):4438–4451
23. Lennartz S, Pisuchpen N, Parakh A et al (2022) Virtual unenhanced images: qualitative and quantitative comparison between different dual-energy CT scanners in a patient and phantom study. Invest Radiol 57(1):52–61
24. Baliyan V, Kordbacheh H, Parameswaran B, Ganeshan B, Sahani D, Kambadakone A (2018) Virtual monoenergetic imaging in rapid kVp-switching dual-energy CT (DECT) of the abdomen: impact on CT texture analysis. Abdom Radiol (NY) 43(10):2693–2701
25. Chatterjee A, Valliéres M, Forghani R, Seuntjens J (2021) Investigating the impact of the CT Hounsfield unit range on radiomic feature stability using dual energy CT data. Phys Med 88:272–277
26. Euler A, Laqua FC, Cester D et al (2021) Virtual monoenergetic images of dual-energy ct-impact on repeatability, reproducibility, and classification in radiomics. Cancers (Basel) 13(18):4710
27. Atwi NE, Smith DL, Flores CD (2019) Dual-energy CT in the obese: a preliminary retrospective review to evaluate quality and feasibility of the single-source dual-detector implementation. Abdom Radiol (NY) 44(2):783–789
28. Darras KE, McLaughlin PD, Kang H et al (2016) Virtual monoenergetic reconstruction of contrast-enhanced dual energy CT at 70keV maximizes mural enhancement in acute small bowel obstruction. Eur J Radiol 85(5):950–956
29. Matsumoto K, Jinzaki M, Tanami Y, Ueno A, Yamada M, Kuribayashi S (2011) Virtual monochromatic spectral imaging with fast kilovoltage switching: improved image quality as compared with that obtained with conventional 120-kVp CT. Radiology 259(1):257–262
30. Berenguer R, Pastor-Juan MDR, Canales-Vázquez J et al (2018) Radiomics of CT features may be nonreproducible and redundant: influence of CT acquisition parameters. Radiology 288(2):407–415
31. Fornacon-Wood I, Mistry H, Ackermann CJ et al (2020) Reliability and prognostic value of radiomic features are highly dependent on choice of feature extraction platform. Eur Radiol 30(11):6241–6250
32. Sullivan DC, Obuchowski NA, Kessler LG et al (2015) RSNA-QIBA Metrology Working Group. Metrology standards for quantitative imaging biomarkers. Radiology 277(3):813–825
33. Bland JM, Altman DG (1999) Measuring agreement in method comparison studies. Stat Methods Med Res 8(2):135–160
34. Reed GF, Lynn F, Meade BD (2002) Use of coefficient of variation in assessing variability of quantitative assays. Clin Diagn Lab Immunol 9(6):1235–1239
35. Bonett DG (2006) Confidence interval for a coefficient of quartile variation. Comput Stat Data Anal 50(11):2953–2957
36. Koo TK, Li MY (2016) A guideline of selecting and reporting intraclass correlation coefficients for reliability research. J Chiropr Med 15(2):155–163
37. Lin LI (1989) A concordance correlation coefficient to evaluate reproducibility. Biometrics 45(1):255–268
38. Lin LI (2000) A note on the concordance correlation coefficient. Biometrics 56(1):324–325
39. Balagurunathan Y, Kumar V, Gu Y et al (2014) Test–retest reproducibility analysis of lung CT image features. J Digit Imaging 27:805–823
40. Segal E, Sirlin CB, Ooi C et al (2007) Decoding global gene expression programs in liver cancer by noninvasive imaging. Nat Biotechnol 25:675–680
41. Tu SJ, Chen WY, Wu CT (2021) Uncertainty measurement of radiomics features against inherent quantum noise in computed tomography imaging. Eur Radiol 31(10):7865–7875
42. Le EPV, Rundo L, Tarkin JM et al (2021) Assessing robustness of carotid artery CT angiography radiomics in the identification of culprit lesions in cerebrovascular events. Sci Rep 11(1):3499
43. Dunning CAS, Rajendran K, Fletcher JG, McCollough CH, Leng S (2022) Impact of improved spatial resolution on radiomic features using photon-counting-detector CT. Proc SPIE Int Soc Opt Eng 12032:1203221
44. D'Angelo T, Cicero G, Mazziotti S et al (2019) Dual energy computed tomography virtual monoenergetic imaging: technique and clinical applications. Br J Radiol 92(1098):20180546
45. Albrecht MH, Vogl TJ, Martin SS et al (2019) Review of clinical applications for virtual monoenergetic dual-energy CT. Radiology 293(2):260–271
46. Zhong J, Xia Y, Chen Y et al (2023) Deep learning image reconstruction algorithm reduces image noise while alters radiomics features in dual-energy CT in comparison with conventional iterative reconstruction algorithms: a phantom study. Eur Radiol 33(2):812–824
47. Ger RB, Zhou S, Chi PM et al (2018) Comprehensive investigation on controlling for CT imaging variabilities in radiomics studies. Sci Rep 8(1):13047
48. Song Y, Zhang J, Zhang YD et al (2020) FeAture Explorer (FAE): a tool for developing and comparing radiomics models. PLoS One 15(8):e0237587
49. Foy JJ, Al-Hallaq HA, Grekoski V et al (2020) Harmonization of radiomic feature variability resulting from differences in CT image acquisition and reconstruction: assessment in a cadaveric liver. Phys Med Biol 65(20):205008
50. Ligero M, Jordi-Ollero O, Bernatowicz K et al (2021) Minimizing acquisition-related radiomics variability by image resampling and batch effect correction to allow for large-scale data analysis. Eur Radiol 31(3):1460–1470
51. Beaumont H, Iannessi A, Cucchi JM, Bertrand AS, Lucidarme O (2022) Intra-scan inter-tissue variability can help harmonize radiomics features in CT. Eur Radiol 32(2):783–792

52. Ibrahim A, Barufaldi B, Refaee T et al (2022) MaasPenn radiomics reproducibility score: a novel quantitative measure for evaluating the reproducibility of CT-based handcrafted radiomic features. Cancers (Basel) 14(7):1599
53. Bertolini M, Trojani V, Botti A et al (2022) Novel harmonization method for multi-centric radiomic studies in non-small cell lung cancer. Curr Oncol 29(8):5179–5194
54. Soliman MAS, Kelahan LC, Magnetta M et al (2022) A framework for harmonization of radiomics data for multicenter studies and clinical trials. JCO Clin Cancer Inform 6:e2200023
55. Li Y, Reyhan M, Zhang Y et al (2022) The impact of phantom design and material-dependence on repeatability and reproducibility of CT-based radiomics features. Med Phys 49(3):1648–1659

Publisher's Note